

DESIGN AND ANALYSIS OF UNIVERSAL COUPLING IN POWER TRANSMISSION

G. RAMESH

14R31D0403, M.Tech

Nova College Of Engineering And Technology
Jafferguda, Hayatnagar, Hyderabad

B.SWATHI

Assistant Professor

Nova College Of Engineering And Technology
Jafferguda, Hayatnagar, Hyderabad

ABSTRACT

Universal joint in a rigid rod that allows the rod to bend in any direction, and is commonly used in shafts that transmit rotary motion. It consists of a pair of hinges located close together, oriented at 90° to each other, connected by a cross shaft. The Universal coupling saves the Gear arrangements cost for making misalign to align torque transmission, decreases the work space for transmitting arrangements. Main problem arises in universal coupling is due to failures which maybe manufacturing and design fault, shear failure, improper assembly, raw material faults, maintenance faults, material processing faults, drivable joint angle, cyclic load ,wear, noise etc. Main objectives are to reduce shear failures by Modification of pin (cross) in existing design of universal coupling. The modeling of proposed design is to be done by using CREO software & static and dynamic analysis is to be done in ANSYS software & results are compared with existing design.

The power produced from an engine of automobile can be transferred to the drive wheel by power transmission system. Each automobile has different power transmission system constructive features depend on the vehicle's driveline concept. (H.Bayrakceken et al., 2006) To transmit the driving torque from the engine or gear unit to the wheels, most of passenger car and light vehicle driven by combustion engine has at least two driveshaft as a basic requirement (Amborn, P. 1995). During operation, torsional stress and bending stress was experienced by driveshaft due to the weight of the car or misalignment of journal bearing (Asi, 2006). In order to meet the requirements of one of the most highly stressed components in automotive assembly, a failure investigation must be conducted. Finite element method was used as stress analysis to determine the stress conditions at the failed section.

Nearly all of driveshaft are metal shafts or metal tubes that has special joint at each end called universal joint (Birch and Rockwood2005).

Power transmission system of vehicles consist several components which sometimes encounter unfortunate failures. Some common reasons for the failures may be manufacturing and design faults, maintenance faults, raw material faults, material processing faults as well as the user originated faults. In this study, fracture analysis of a universal joint yoke and a drive shaft of an automobile power transmission system are carried out. Spectroscopic analyses, metallographic analyses and hardness measurements are carried out for each part. For the determination of stress conditions at the failed section, stress analysis is also carried out by the finite element method. The common failure types in automobiles and revealed that the failures in the transmission system elements cover 1/4 of all the automobile failures. Some common reasons for the failures may be manufacturing and design faults, maintenance faults, raw material faults as well as the user originated faults. This paper presents FEM analysis of universal coupling with the help of ANSYS for different torque or load condition and it verify by manual calculation.

Keywords — Universal Coupling, CREO, ANSYS , Assembly, Strain, Stress

INTRODUCTION

In day-to-day life every aspect is influenced by the work of engineer. The equipment's we use, the food we eat, and the vehicles we travel in and many more all are developed with the assistance of design engineering. Traditional design has been done by simple calculation. But with

increase in product performance and reliability it is difficult to follow the traditional iterative design procedures. As product performance becomes more important and as designs become more complex the simple method has become inadequate. To understand the growth and its implication for design, it is necessary to look at how design solutions are implemented. To satisfy the market needs it is necessary to provide a computational capacity along with the creativity of the human being. By adding computer technology to the armory of the designer, the best qualities of the designer can be linked with the best qualities of the computer. Most engineering designs are too complex for traditional approach. For example a structure may have spatially dependent material properties if different materials are used; the geometry may be irregular in some sense or the boundary condition may be complex. In all these examples no solution functions exist and so solutions can be achieved only by resorting to an approximate numerical method. A widely used numerical method for solving structural problems in both industry and academia is "FINITE.

The purpose of a steering system is to control the direction of the vehicle by operating the steering wheel of the steering system. Movement of steering wheel by the driver should cause an accurate response of the road wheels. The intermediate shaft connects the steering shaft to the steering pinion. These components cannot be arranged on the same axis due to the vehicle design limitations. They are arranged with the universal joints. The stresses in either direction, while moving the vehicle to the

right or to the left, happen to be a source of failure of the mechanical joint. The two halves of the yoke, the web connecting the two halves or the shaft in the linkages are prone to failure. In such event, the driver could lose control leading to an accident.

A universal joint also known as universal coupling, U joint, Cardan joint, Hardy-Spicer joint, or Hooke's joint is a joint or coupling used to connect rotating shafts that are coplanar, but not coinciding. A universal joint is a positive, mechanical connection used to transmit motion, power or both. Each universal joint assembly consists of three major components: two yokes (flange and weld) and a cross trunnion. An automotive flange yoke has a machined flat face which may be affixed through a bolted connection to the rear differential of a vehicle. A weld yoke incorporates a machined step, and is inserted into the end of the driveshaft and welded in place. The cross trunnion is used to deliver rotation from one yoke to another using four needle pin bearings.



Typical Universal coupling

Modelling of the component ProE(creo3.0) software is used. Pre-processing work like meshing and analysis

work is carried out in HYPERWORKS software. Using FEA analysis, we can identify the nature and characteristics of stresses acting on the yoke and evaluate the influence of the load/mass geometry/boundary conditions over the yoke. Fig shows the 2D model geometry of benchmark yoke assembly.

Literature Review

Bell's Inequality [1] was derived by John Bell in 1964 as a response to The Einstein-Podolsky-Rosen Paradox [2], a problem pertaining to the foundations of quantum physics. Bell saw his inequality as being able to discern between two different epistemological views of quantum mechanics, the one proposed by EPR and the one proposed by the Copenhagen interpretation of quantum theory.

In this paper we point out another implication of Bell's work. We first derive a coupling principle directly from the inequality and show that the Pauli principle can be viewed as a special case of this coupling. We then apply the principle to further our understanding of baryonic structure and note that the case of spin $3/2$ baryons can be analyzed in one of two ways as reflected in the following assumptions:

- (1) In every direction the spin will be observed to be $3=2$.
- (2) There exists some direction in which the spin will be observed to be $3=2$. Assumption (1) in fact is the key point of a previous paper [6] and will not be discussed here. Assumption (2), on the other hand, when combined with the coupling principle mentioned above, enables us to explain the

statistical structure of the and the Ω particles without any recourse to color. It is discussed in section four of the paper.

A Coupling Principle

Consider three (or more) particles in the same spin state. In other words, if a measurement is made in an arbitrary direction a_1 on ONE of the three particles, then the measurements can be predicted with certainty for the same direction for each of the other particles. We point out immediately that such spin correlations are isotropic for the particles under discussion and that we are not dealing with a polarization phenomenon where spin correlations exist for a preferred direction. In our case, the particles are spin-correlated in all directions at once, as for example in the case of two particles in a singlet state. Hence, the initial direction of measurement is arbitrary. We refer to such particles as isotopically spin-correlated particles. Specially, if we denote a spin up state by the ket j

$+ \rangle$ and a spin down state by the ket $j \rightarrow$ then without loss of generality, we can assume that the three particles have the joint spin state $J +; +; + \rangle (j \rightarrow; -; - \rangle)$, where the suffix 1, refers to the observed spin states in the arbitrary direction a_1 .

In the language of probability, we can say that if the spin state of a particle is $j \rightarrow$ 1 then the corresponding spin state of each of the other two particles can be predicted (for the same direction) with probability 1. Furthermore, the probability 1 condition means that in principle spin can now be measured simultaneously in the three different directions $a_1; a_2; a_3$, for the three

particle ensemble (see Fig. 1). Let P denote the joint probability measure relating the measurements in the three different directions and recall the fact that if spin is observed to be in the $j \rightarrow 1$ state in direction a_1 for one of the particles then the conditional probability of observing $j \rightarrow 2$ or $j \rightarrow 3$ in the direction a_2 for a second particle, is given by $\cos^2(\theta_{12})$ or $\sin^2(\theta_{12})$ respectively, where θ_{12} is the angle subtended by a_1 and a_2 and c is a constant. For the purpose of the argument below, we will work with $c = 1/2$. However, the argument can be made to work for any value of c , and in a particular way can be applied to the spin of a photon, provided $c = 1/2$.

With notation now in place, we adapt an argument of Wigner [4] to show that isotopically spin-correlated particles must occur in pairs. We prove this by contradiction. Specially, consider three isotopically spin-correlated particles (see Fig. 2.1), as explained above. It follows from the probability 1 condition, that three spin measurements can be performed, in principle, on the three particle system, in the directions $a_1; a_2; a_3$. Let $(s_1; s_2; s_3)$ represent the observed spin values in the three different directions. Note that $s_i = \pm 1$ in the notation developed above which means that there exists only two possible values for each measurement. Hence, for three measurements there are a total of 8 possibilities in total. In particular,

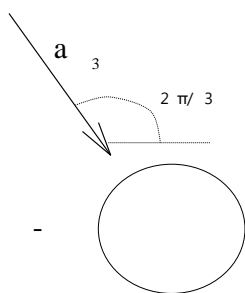


Figure 2.1 Three isotopically spin-correlated

$$\{(+, +, -), (+, -, -)\} \subset \{(+, +, -), (+, -, -), (-, +, -), (+, -, +)\}$$

$$P\{(+, +, -), (+, -, -)\} \leq P\{(+, +, -), (+, -, -), (-, +, -), (+, -, +)\}.$$

Therefore,

$$\frac{1}{2} \sin^2 \frac{\theta_{31}}{2} \leq \frac{1}{2} \sin^2 \frac{\theta_{23}}{2} + \frac{1}{2} \sin^2 \frac{\theta_{12}}{2}.$$

If we take $\theta_{12} = \theta_{23} = \frac{\pi}{3}$ and $\theta_{31} = \frac{2\pi}{3}$ then this gives $\frac{1}{2} \geq \frac{3}{4}$ which is clearly a contradiction. In other words, three particles cannot all be in the same spin state with probability 1, or to put it another way, isotopically spin-correlated particles must occur in pairs.

Finally, as noted above, this argument applies also to spin 1 particles, like the photons, provided full angle formulae are used instead of the half-angled formulae.

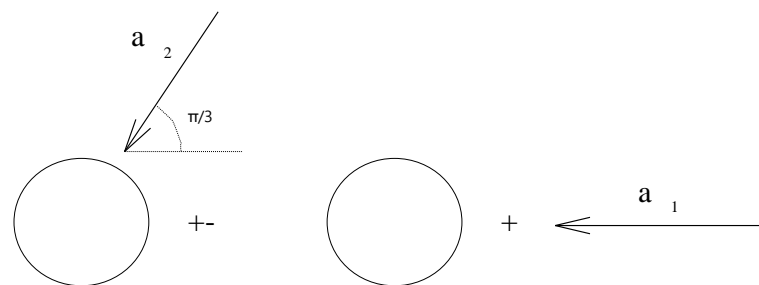
2.3 Pauli Exclusion Principle

The above results can be cast into the form of a theorem (already proven above) which will be referred to as the “coupling principle”.

Theorem 1 (*The Coupling Principle*) *Isotopically spin-correlated particles must occur in PAIRS.*

In practice, isotopically spin-correlated particles occur when the particles’ spin are either anti-parallel (singlet state) or parallel to each other.

We now show that when a system of indistinguishable particles contain “coupled”



particles then this system of particles must obey fermi-dirac statistics. We first do this for a 2- particle spin-singlet state system and then extend the result to an nparticle system. Throughout $\lambda_i = (q_i, s_i)$ will represent the quantum coordinates of particle i, with s_i referring to the spin coordinate and q_i representing all other coordinates. In practice, $\lambda_i = (q_i, s_i)$ will represent the eigenvalues of an operator defined on the Hilbert space $L^2(\mathbb{R}^3) \otimes H_2$, where H_2 represents a two-dimensional spin space of particle i. We will mainly work with λ_i . However, occasionally, in the interest of clarity, we will have need to distinguish the q_i from the s_i .

Corollary 1 Let $|\psi(\lambda_1, \lambda_2)\rangle$ denote a two particle state where the λ_1 and λ_2 are as defined above. If the particles are in a spin-singlet state then their joint state function will be given by

$$|\psi_i(\lambda_1, \lambda_2)\rangle = \frac{1}{\sqrt{2}} [|\psi_1(\lambda_1)\rangle \otimes |\psi_2(\lambda_2)\rangle - |\psi_1(\lambda_2)\rangle \otimes |\psi_2(\lambda_1)\rangle]$$

In other words, coupled particles obey fermi-dirac statistics.

Proof: The general form of the two particle eigenstate is of the form

$$|\psi(\lambda_1, \lambda_2)\rangle = c_1 |\psi_1(\lambda_1)\rangle \otimes |\psi_2(\lambda_2)\rangle + c_2 |\psi_1(\lambda_2)\rangle \otimes |\psi_2(\lambda_1)\rangle$$

Since the particles are in a spin-singlet state then $P(\lambda_1 = \lambda_2) \leq P(s_1 = s_2) = 0$. Therefore, $\langle \psi(\lambda_1, \lambda_1) | \psi(\lambda_1, \lambda_1) \rangle = 0$ and hence $|\psi(\lambda_1, \lambda_1)\rangle = 0$, from the inner product properties of a Hilbert space. It follows, that $c_1 = -c_2$ when the particles are coupled and normalizing the wave function gives $|c_1| = \frac{1}{\sqrt{2}}$. The result follows. QED

Note that the same result can also be used to describe particles whose spin

correlations are parallel to each other in each direction. This can be done by correlating a measurement in direction a on one particle, with a measurement in direction $-a$ in the other. In this case, the state vector for the parallel and anti-parallel measurements will be found to be by the above argument:

$$|\psi(\lambda_1, \lambda_2)\rangle = \frac{1}{\sqrt{2}} [|\psi_1(\lambda_1)\rangle \otimes |\psi_2(\lambda_2(\pi))\rangle - |\psi_1(\lambda_2)\rangle \otimes |\psi_2(\lambda_1)\rangle]$$

where the π expression in the above arguments, refer to the fact that the measurement on particle two is made in the opposite sense, to that of particle one.

This result can now be generalized to derive the Pauli Exclusion Principle for a system of n indistinguishable particles containing an least one pair of coupled particles. First, note the following use of notation. Let $|\psi_i(\lambda_j)\rangle = \psi_i(\lambda_j) \sim e$ where $\psi_i(\lambda_j)$ refers to particle i in the state $|\psi_i(\lambda_j)\rangle$ and $\sim e$ is a unit vector. Then

$$|\psi_i(\lambda_j)\rangle \otimes |\psi_k(\lambda_l)\rangle = [\psi_i(\lambda_j) \sim e_1] \otimes [\psi_k(\lambda_l) \sim e_2] = \psi_i(\lambda_j) \psi_k(\lambda_l) \sim e_1 \otimes e_2 = |\psi_k(\lambda_l)\rangle \otimes |\psi_i(\lambda_j)\rangle$$

In other words, the tensor product is commutative. From now on we will drop the ket notation and simply write that $\psi_i(\lambda_j) \otimes \psi_k(\lambda_l) = \psi_k(\lambda_l) \otimes \psi_i(\lambda_j)$, with ket notation being understood. We also denote an n-particle state by $\psi_{1\dots n}[\lambda_1, \dots, \lambda_n]$ where the subscript $1\dots n$ refer to the n particles.

However, when there is no ambiguity involved we will simply write this n-particle state as $\psi[\lambda_1, \dots, \lambda_n]$ with the subscript $1 \dots n$ being understood. Finally, note that for an indistinguishable system of n particles

$$\psi[\lambda_1, \dots, \lambda_n] = X_{\sigma_P} C_P \psi(\lambda_1, \dots, \lambda_n)$$

where $\psi(\lambda_1, \dots, \lambda_n) = \psi_1(\lambda_1) \otimes \dots \otimes \psi_n(\lambda_n)$ and $\sigma_P (\psi_1 \otimes \dots \otimes \psi_n) = \psi_{i1} \otimes \dots \otimes \psi_{in}$, gives a permutation of the states. With this notation, we now prove the following theorem:

Theorem 2 (The Pauli Exclusion Principle)

A sufficient condition for a system of n indistinguishable particles to exhibit fermi-dirac statistics is that it contain spin-coupled particles .

Proof: We will work with three particles, leaving the general case for the Appendix. Consider a system of three indistinguishable particles, containing spin-coupled particles. Using the above notation and applying Cor 1 in the second line below, we can write:

$$\begin{aligned} \psi[\lambda_1, \lambda_2, \lambda_3] &= \frac{1}{\sqrt{3}} \{ \psi_1(\lambda_3) \otimes \psi_{23}[\lambda_1, \lambda_2] + \psi_2(\lambda_3) \otimes \psi_{13}[\lambda_1, \lambda_2] + \psi_3(\lambda_3) \otimes \psi_{12}[\lambda_1, \lambda_2] \} \\ &= \frac{1}{\sqrt{3!}} \{ \psi_1(\lambda_3) \otimes [\psi_2(\lambda_1) \otimes \psi_3(\lambda_2) + \psi_2(\lambda_3) \otimes [\psi_3(\lambda_1) \otimes \psi_1(\lambda_2) - \psi_3(\lambda_3) \otimes [\psi_1(\lambda_1) \otimes \psi_2(\lambda_2) - \psi_1(\lambda_3) \otimes \psi_2(\lambda_1)]] \} \\ &= \sqrt{3!} \psi_1(\lambda_1) \wedge \psi_2(\lambda_2) \wedge \psi_3(\lambda_3) \end{aligned}$$

where \wedge represents the wedge product. Thus the wave function for the three indistinguishable particles obeys the fermi-dirac statistics. The n-particle case follows by induction. QED.

Mathematically it is possible to give other reasons why $P(\lambda_i, \lambda_i) = 0$ (quark “color” being a case in point) In fact, a necessary and sufficient condition can be formulated for fermi-dirac statistics as follows: In a system of n- indistinguishable particles

$\psi[\lambda_1, \dots, \lambda_i, \lambda_i, \dots] = 0$ for the i and j states if and only if

$$\psi[\lambda_1, \lambda_2, \dots, \lambda_n] = \sqrt{n!} \psi_1(\lambda_1) \wedge \psi_2(\lambda_2) \wedge \dots \wedge \psi_n(\lambda_n)$$

The sufficient part of the proof will be the same as in Theorem 2 while the necessity part is immediate. However, the significance of Theorem 2 lies in the fact that for spin-type systems, particles may couple and this coupling causes fermi-dirac statistics to occur. Moreover, the coupling would appear to be a more universal explanation of the Pauli exclusion principle than for example “color”. Not only does it explain the statistical structure of the baryons (see below) but it also explains why in chemistry only two electrons share the same orbital and why “pairing” occurs in the theory of superconductivity.[3],[5, p8]

MODELING OF UNIVERSAL COUPLING

INTRODUCTION OF PTC CREO PARAMETRIC 3.0

PTC Creo Parametric, developed by Parametric Technology Corporation, is a new technology in the series of Pro/ENGINEER. It provides a broad range of powerful and flexible CAD capabilities that can address even the most tedious design challenges. Being a parametric feature-based solid modeling tool, it not only integrates the 3D parametric features with 2D tools, but also assists in every design-through-manufacturing process. This software is remarkably user-friendly and it contributes to the enhanced of the entire design process.

This solid modeling software allows you to easily import the standard

format files with an amazing compatibility. The 2D drawing views of the components are automatically generated in the **Drawing** mode. Using this software, you can generate detailed, orthographic, isometric, auxiliary, and section views. Additionally, you can use any predefined drawing standard files for generating the drawing views. You can display the model dimensions in the drawing views or add reference dimensions whenever you want. The bidirectional associative nature of this software ensures that any modification made in the model is automatically reflected in the drawing views. Similarly, any modification made in the dimensions of the drawing views is automatically updated in the model.

The **PTC Creo Parametric 3.0 for Engineers and Designers** textbook has been written to enable the readers to use the modeling power of PTC Creo Parametric 3.0 effectively. The latest surfacing techniques like Freestyle and Style are explained in detail in this book. The textbook also covers the Sheet metal module with the help of relevant examples and illustrations. The mechanical engineering industry examples and tutorials are used in this textbook to ensure that the users can relate the knowledge of this book with the actual mechanical industry designs. The salient features of this textbook are as follows:

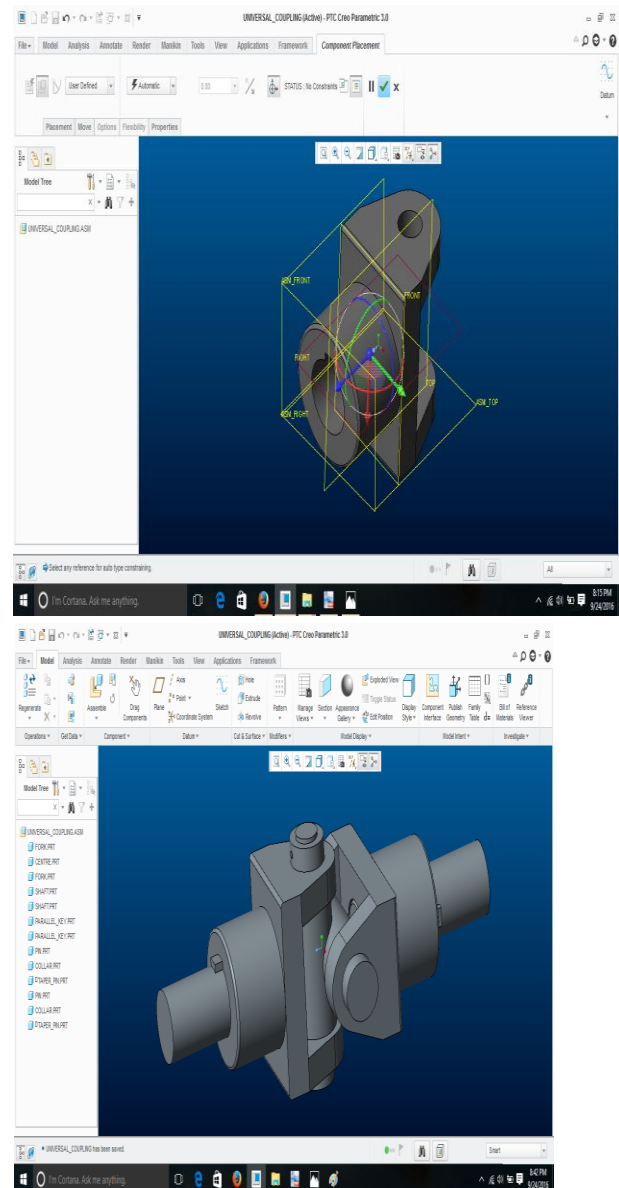
Modeling steps of universal coupling

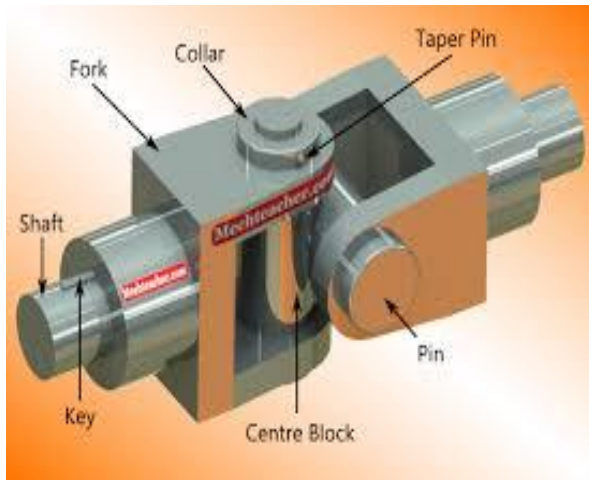
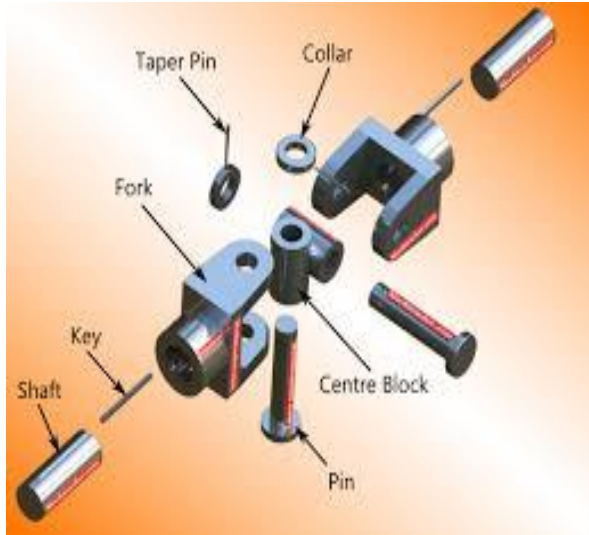
4.3.1 Fork: The fork is one of the part of universal coupling. As per the drawing need to create part modeling by using creo 3.0.

The dimensions are as per production drawing need to maintain.

- Modules using in this part
 - ❖ Sketching
 - ❖ Part Modeling
 - ❖ Assembly
- Material: Cast Steel

As per the 2D drawing need to create 3D modeling.





ANALYSIS OF UNIVERSAL COUPLING

The purpose of a steering system is to control the direction of the vehicle by operating the steering wheel of the steering system. Movement of steering wheel by the driver should cause an accurate response of the road wheels. The intermediate shaft connects the steering shaft to the steering pinion. These components cannot be arranged on the same axis due to the vehicle design limitations. They are arranged with the universal joints. The stresses in either direction, while moving the vehicle to the right or to the left, happen to be a source of

failure of the mechanical joint. The two halves of the yoke, the web connecting the two halves or the shaft in the linkages are prone to failure. In such event, the driver could lose control leading to an accident.

A universal joint also known as universal coupling, U joint, Cardan joint, Hardy-Spicer joint, or Hooke's joint is a joint or coupling used to connect rotating shafts that are coplanar, but not coinciding. A universal joint is a positive, mechanical connection used to transmit motion, power or both. Each universal joint assembly consists of three major components: two yokes (flange and weld) and a cross trunnion. An automotive flange yoke has a machined flat face which may be affixed through a bolted connection to the rear differential of a vehicle. A weld yoke incorporates a machined step, and is inserted into the end of the driveshaft and welded in place. The cross trunnion is used to deliver rotation from one yoke to another using four needle pin bearings.

Modelling of the component ProE software is used. Pre-processing work like meshing and analysis work is carried out in ANSYS software. Using FEA analysis, we can identify the nature and characteristics of stresses acting on the yoke and evaluate the influence of the load/mass geometry/boundary conditions over the yoke. Fig shows the 2D model geometry of benchmark yoke assembly.

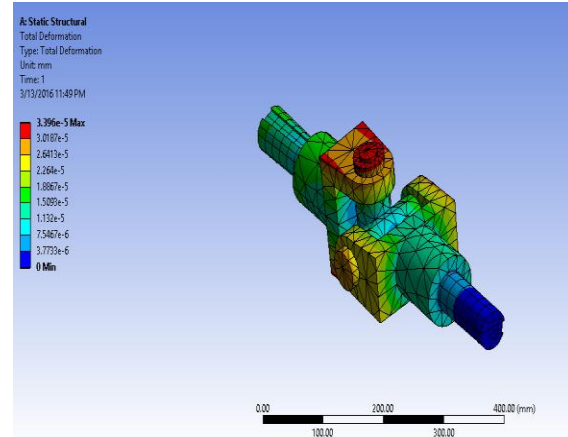
ANALYSIS IN ANSYS SOFTWARE

After modeling in CREO software, triangular type of meshing of hub, pin & assembly is done

in ANSYS software. In hub number of elements are 6033 & number of nodes are 10904

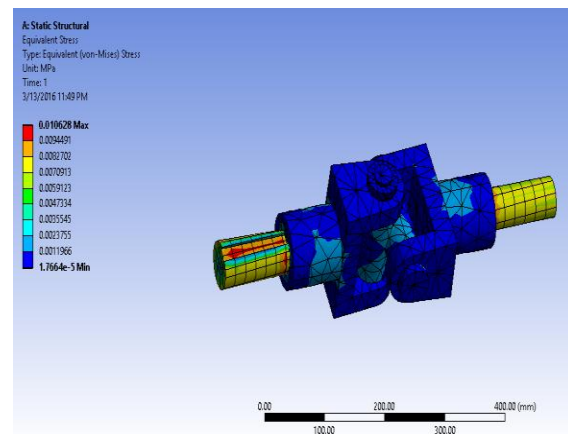
Complete a study by performing the following steps:

- Create a study defining its analysis type and options.
- If needed, define parameters of your study. Parameters could be a model dimension, a material property, a force value, or any other entity that you want to investigate its impact on the design.
- Define material properties. This step is not required in COSMOS Works if material properties were defined in CREO 3.0.
- Specify restraints. For example, in structural studies you define how the model is supported.
- Specify the loads.
- Mesh the model where COSMOS Works divides the model into many small pieces called elements.
- Link the parameters to the appropriate study inputs.
- Define as many design scenarios as you want (up to 100 design scenarios).
- Run the study or selected design scenarios.
- View and list the results



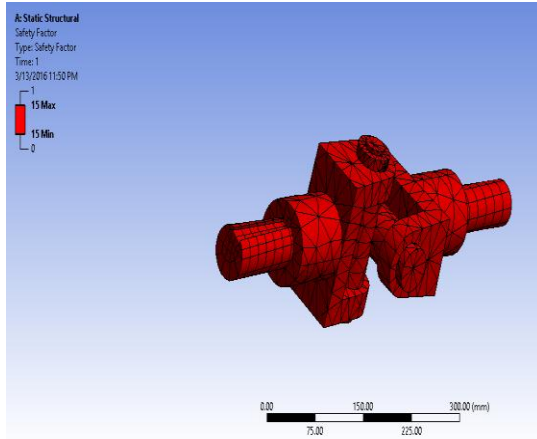
Deformation of universal coupling

Deformation of universal coupling is analyzed in ANSYS Software. The maximum value of deformation in universal coupling is 3.396e MPa & minimum value is of 0 MPa.



Stress Analysis of universal coupling

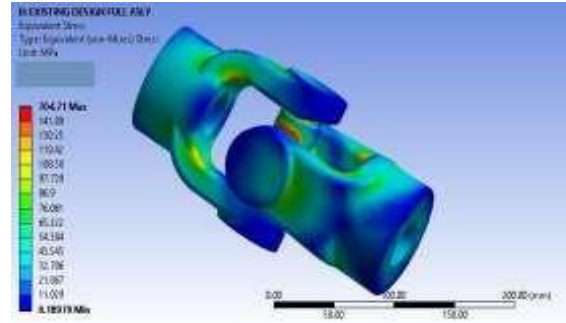
As shown in figure 5.15 Stress Analysis of universal coupling is analyzed in ANSYS Software. The maximum value of Stress Analysis in universal coupling is 0.010628 MPa & minimum value is of 1.7664e-5 MPa



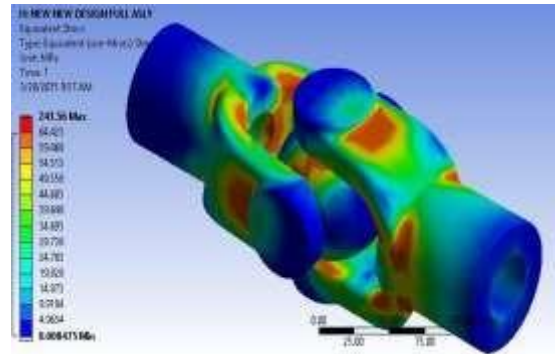
Safety Factor of universal coupling
COMPARISON BETWEEN EXSITING DESIGN & PROPOSED DESIGN

Stress analysis of existing design is ANSYS is done which is shown in figure 5.17. Whole assembly of proposed design is analyzed for stress analysis which is shown in figure 5.18

In existing design von mises stress is 704.21 MPa. By comparing existing design with proposed design stress value is decreased from 704.21 MPa to 241.56 MPa.



Stress Analysis Of Existing Design



Stress Analysis Of Proposed Design

Comparison				
Existing Design And Proposed Design Analysis Data For Von Mises Stress				
Sr	Part / Assembly Name	Existing Design	Proposed Design	Difference
1	Full Assembly Stress	704.71	241.56	463.15
2	Hub Stress	46.19	42.67	3.52
3	Pin / Ball Stress	23101	5980.3	17120.7

The shear stress analysis for existing design is of 351.3 MPa . Shear stress for proposed design is 120.04 MPa Hence shear stress is reduced in proposed design of universal coupling.

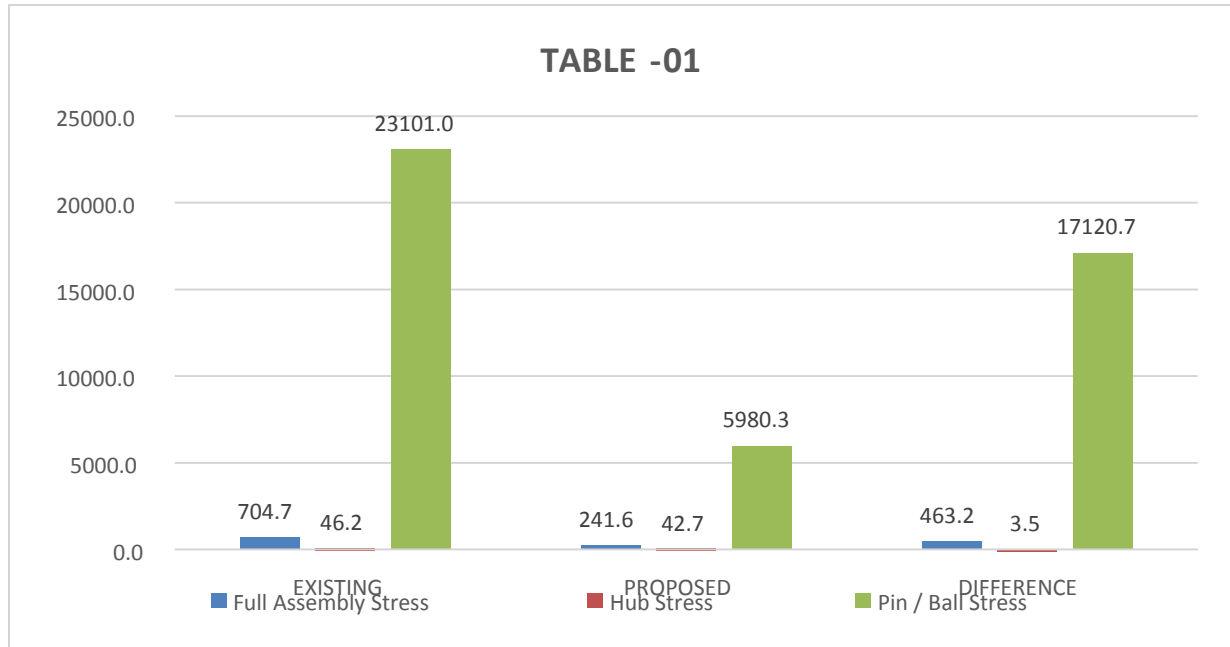
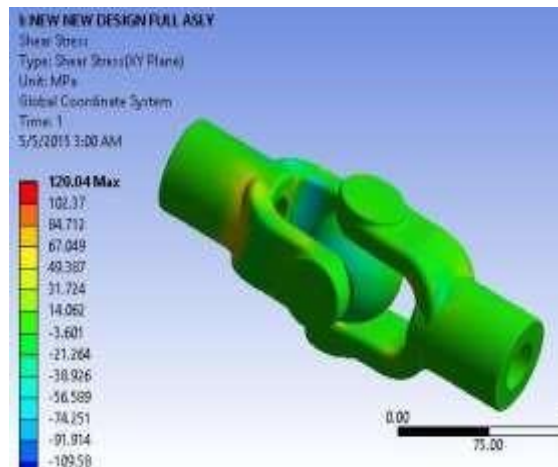
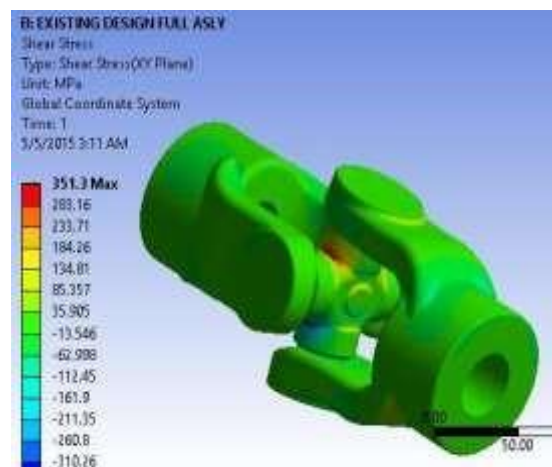


Chart 1 Comparison of Existing Design & Proposed Design - Analysis Data For Von Mises Stress



Shear Stress Analysis-Existing Design



Shear Stress Analysis-Proposed Design

Comparison					
Existing Design And Proposed Design Analysis Data For Shear Stress					
Sr	Part / Assembly Name	Existing Design	Proposed Design	Difference	
1	Full Assembly Stress	351.3	120.04	231.26	
2	Hub Stress	23.41	21.63	1.78	
3	Pin / Ball Stress	11507	3530.8	7976.2	

TABLE -02

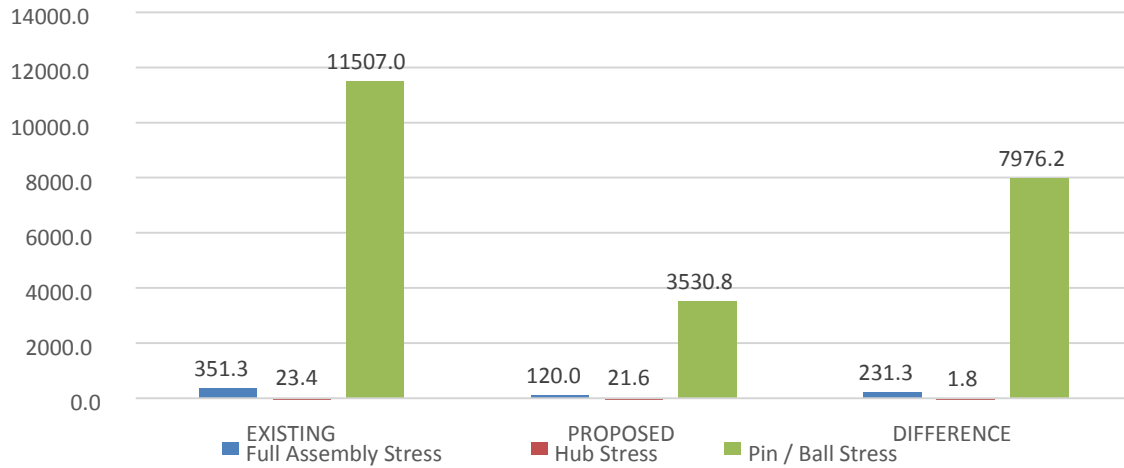


Chart 2 Comparison of Existing Design & Proposed Design - Analysis Data For Shear Stress Moment Applied To Proposed Assembly

DYNAMIC ANALYSIS

Power is of 90KW & universal coupling rotate at 250 RPM. So torque is find out by the

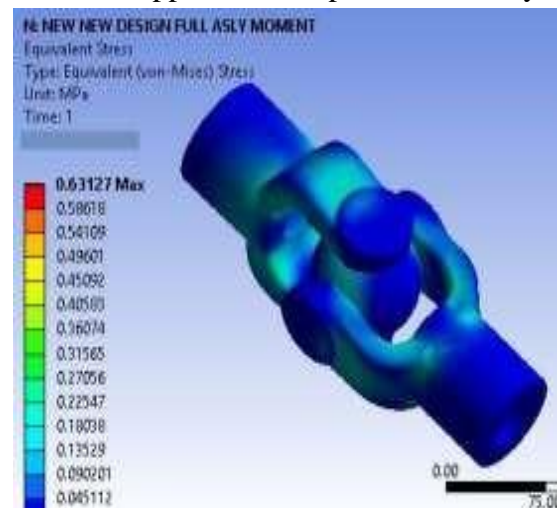
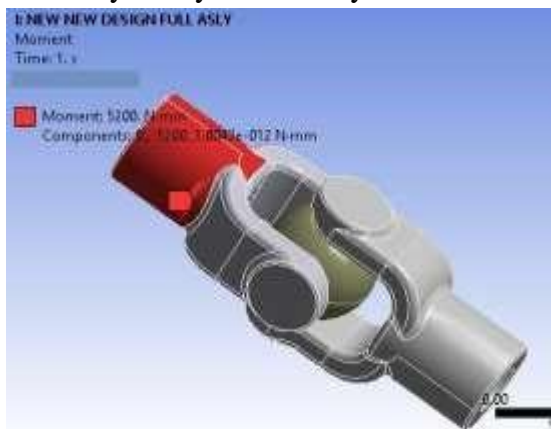
Use of Equation as mentioned below for dynamic analysis purpose. The factor of safety 1.5 is considered.

$$T = \frac{P \times 60}{2\pi N}$$

$$= \frac{90 \times 10^3 \times 60}{(2\pi \times 250)}$$

$$= 3440 \times 10^3 \text{ N-mm}$$

By considering factor of safety of 1.5 , moment 3440*1.5=5200 is applied to the assembly for dynamic analysis



Dynamic Analysis Of Assembly For Stress
The moment of 5200 is applied to whole assembly f proposed design as shown in
By analysis in ANSYS software, maximum stress generated in assembly is of 0.63127 MPa

RESULTS AND DISCUSSION

In our specimen, the material considered is Al 1060 alloy. Modulus of elasticity of the material is E=69 GPa and Poisson's ratio is

$\nu = 0.33$. The simulation has been carried out in room temperature, which is considered to be 25 °C. To find out the most critical condition in terms of stress and strain, the clearance between the hub and the slot of yoke is kept zero.

The generation of strain across the yoke. It is found to be maximum along the edge of the yoke extension. Besides there is also an abrupt rise of strain at the extension-base intersection. The maximum value of strain is found to be 6.2×10^{-5} and the minimum value is found to be 1.93×10^{-8} . The value of strain around the slot is found to be almost 3×10^{-5} .

A demonstration of displacement, takes place during the operation of a universal coupling. The displacement is found to be maximum at the free end of the yoke extension. It is in conformity with the physical condition because the extension works as a cantilever and a cantilever with a load at the free end displays maximum displacement at that end. On the other hand the displacement is negligible at the base. It is also valid because the base is considered to be rigidly fixed. The maximum value of the displacement is found to be almost 0.02mm.

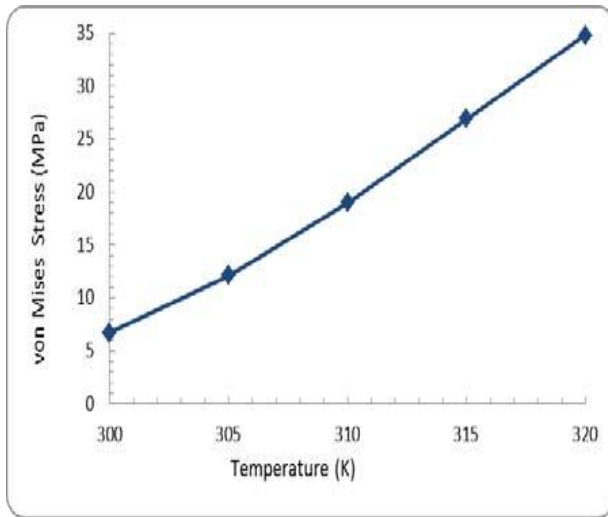
The demonstration of von Mises stress generated in the yoke. Like the generation of strain, maximum stress is found along the edge and at the extension-base intersection of the yoke. The maximum value is found to be 6.03 MPa and the minimum value is found to be almost 0.00099 MPa. Stress around the slot is about 3 MPa, which is half of the maximum stress. So in terms of von Mises stress, the most critical zone of a yoke is the base-

extension intersection and the edge of the yoke extension having the maximum probability to fail. But under the given load at room temperature, the yoke would not fail because the maximum stress is 6.03 MPa which is much smaller than the yield strength of Al 1060 alloy, which again is 27.57 MPa.

Fig. 7.1 shows relationship between temperature at the slot of the yoke and generation of maximum stress in the yoke. With increase of temperature in the slot surface, stress increases across the yoke. The between the hub and the slot of the yoke, the more temperature rise will be, hence the more stress generation will be. The friction can be reduced significantly using bearing and lubricant. From the figure it is evident that under given loading and restrained

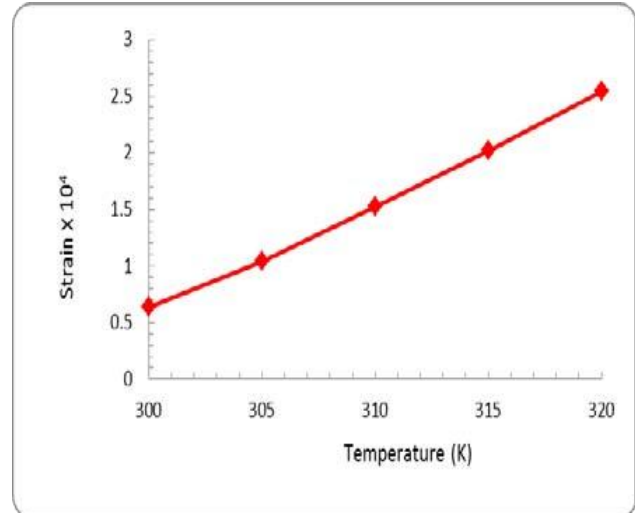
condition, the yoke material will fail if the operating as well as yoke temperature rises as much as 315K (42 °C). Temperature 300K and 305K is almost the same, then there is an abrupt rise in displacement. The relationship is linear in the temperature range between 305K and 320K.

Fig. 11 shows the distribution of von Mises stress in the hub. At the two free ends of the hub, circumferential pressure is applied at the slot-hub interface. The other two ends are assumed to be fixed. From the figure it is evident that, for the same loading condition as like in the yoke, generation



Stress- Temperature relation (load constant) stress in the hub is larger.

In case of yoke, the maximum stress generation is 6.03 MPa, where as in case of hub it is 7.577 MPa, which is about 20.4% larger than the previous one. That means between the yoke and the hub, the hub will fail first, provided that both of them are facing same loading conditions. The extreme failure regions are found at the corners of the hub

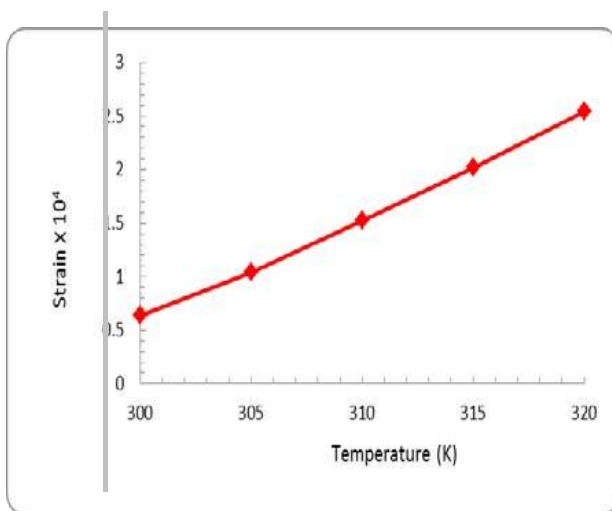


Displacement-Temperature relation (load constant)

A relationship between temperature rise and displacement in the yoke has been showed. The relationship is not linear. The displacement at For example, if the temperature at the slot of the yoke ° increases up to 315K (42 C), the material may yield, because the generated stress will cross the yield strength of Al 1060 alloy

The result obtained are quite favorable which was expected. Finite element method is effectively utilized for addressing the conceptualization and formulation for the design stages. The stresses derived during analysis phase normally indicate the potential solution. The iterations are carried out in the analysis phase which yields the suitable values for design parameter

To improve performance, geometry has been modified using topology and free size optimization which enables to reduce stress level marginally well below the yield limit.



Strain-Temperature relation (load constant)

1. a percent mass reduction of about 7%, is the recommended variant among the alternatives
2. The stress levels observed about 71 MPa in this variant is well within the permissible yield limit of 250 MPa. The distribution of stress too is uniform.
3. Part is safe under given loading condition.

The working stress are less than the yield stress, which improves the design life of yoke

CONCLUSION

In this work design & finite element analysis of universal coupling is carried out. The modelling of proposed design is done by using CREO software & static and dynamic analysis is done in ANSYS software. In existing design von mises stress and shear stress are 704.71 MPa & 351.3 MPa respectively. After the modification in pin's design von mises stress and shear stress are reduced to 241.46 MPa & 120.04 MPa respectively. By the comparison of both the result it is found that the von mises stress is reduced from 704.71MPa to 241.46MPa & shear stress is reduced from 351.3MPa to 120.04MPa. So shear failure is automatically reduced. The failure of component is occur due to manufacturing and design fault, shear failure, improper assembly, raw material faults, maintenance faults, material processing faults, drivable joint angle, cyclic load ,wear, noise etc. The main objective of this work is to reduce shear failure.

The results were obtained are quite favorable which was expected. This result focus the relationship between the manufacturing cost and joint angle performance measures of an automotive universal joint, the results illustrate that an increase in the drivable joint angle requires a corresponding increase in manufacturing cost. However, for both the flange and weld yoke, a substantial reduction in manufacturing cost may be realized by restricting the joint angle to less than 30°. That the manufacturing cost of the flange and weld yokes may be decreased by 4.5% and 4.0%, respectively, while simultaneously increasing the joint angle by 34° and 38°.

REFERENCES

1. S.G.Solanke and A.S.Bharule, "An Investigation On Stress Distribution For Optimization Of Yoke In Universal Joint Under Variable Torque Condition" International Journal of Mechanical Engineering and Robotics Research Vol. 3, No. 2, April 2014 ISSN 2278 – 0149
2. Anup A. Bijagare, P.G. Mehar and V.N. Mujbaile, "Design Optimization & Analysis of Drive Shaft", VSRD International Journal of Mechanical, Auto. & Prod. Engg. Vol.2 (6), 2012.
3. S.K. Chandole, M.D.Shende, M.K. Bhavsar "Structural Analysis of Steering Yoke Of An Automobile for Withstanding Torsion/ Shear Loads", IJRET: International Journal

Of Research in Engineering and
Technology Volume: 03 Issue: 03 | Mar-
2014

4. Farzad Vesali, Mohammad Ali
Rezvani* and Mohammad Kashfi,
“Dynamics of

Universal joints, its failures and some
propositions for practically improving its

Performance and life expectancy”
Journal of Mechanical Science and
Technology 26(8)

(2012) 2439~2449

5. Naik Shashank Giridhar, Sneha
Hetawal and Baskar P., “Finite Element
Analysis of

Universal Joint and Propeller Shaft
Assembly”, International Journal of
Engineering

Trends and Technology (IJETT) -
Nov 2013 – Volume Number 5

6. Sunil Chaudhry, Anil Bansal, Gopal
Krishan “Finite Element Analysis and
Weight

Reduction of Universal Joint using
CAE Tools “International Journal of
Engineering

Research & Technology (IJERT)
ISSN: 2278-0181 Vol. 3 Issue 10, October-
2014

7. P.G. Tathe, Prof. D.S. Bajaj and
Swapnil S. Kulkarni, “Failure Analysis And

Optimization in Yoke Assembly
Subjected By Torsion and Shear”,
International

Journal of Advance Engineering
Research and Studies EISSN2249–8974.
July-

Sept, 2014

8. S.K. Chandole, M.K. Bhavsar, S.S.
Sarode, G.R. Jadhav “Design Evaluation
And

Optimization of Steering Yoke of an
Automobile “International Journal of
Research in

Engineering and Technology | pISSN:
2321-7308 Volume: 03 Issue: 11 | Nov-
2014,

9. Kamal Kashyap, D.G. Mahto “Analysis
of Hooks Joint Using Ansys by Von-

Mises Method” International Journal
of Engineering and Advanced Technology

(IJEAT) ISSN: 2249 – 8958, Volume-
3, Issue-3, February 2014

10. H. Bayrakceken, S. Tasgetiren I.
And Yavuz, “Two cases of failure in

the power transmission system on
vehicles: A universal joint yoke and
a drive shaft”, Engineering Failure
Analysis 14 (2007) 716–724.

11. S. Kinme, T. Kamikawa, A. Nishino,
K. Ikeda and S. Inoue,

“Development of Stamped Yoke for
High Rigidity Intermediate Shaft”
Koyo Engineering Journal English
Edition 165E (2004).